

1 Transient heat transfer

1.1 Introduction

With respect to heat transfer, up to now the focus has been restricted to those systems and bodies whose temperature does not depend on time, that is to say where $\partial T/\partial t = 0$, and there are many instances where this steady-state assumption is reasonable. However, in general, the temperature more often than not varies in time as well as in space. Take, as a light-hearted example, the process of boiling an egg. It can often be quite a contentious, and highly personal, issue as to what constitutes a ‘good’ boiled egg. Whether you prefer the centre to be silky soft or rock hard, the length of time that the egg is cooked for plays a central role and clearly in this situation we have a body (the egg) whose temperature is not constant over time. When it comes to cooking, the desired outcomes are most often arrived at through a process of trial and error but being engineers, not chefs, we may prefer to ask if there is a more objective approach that can be taken to predicting the behaviour of our system of interest. The answer, of course, is yes and attention will now be centred around those methods that can be applied to solving these types of ***transient*** (or ***unsteady***) problems.

Following this short introduction, three such methods will be discussed and they are presented in order of the complexity of problem that they can be used to solve. We start with the simplest case of ***lumped system analysis*** where the temperature is considered to be a function of time alone i.e. $T(t)$. We will also see that the range of applicability of this approach is quite limited so we then progress to more sophisticated ***analytical methods*** where temperature varies not only in time but also in one spatial dimension i.e. $T(x, t)$. The section closes with a brief introduction to ***numerical methods*** and while in principle we can apply these to solve fully three-dimensional transient problems i.e. $T(x, y, z, t)$ here, due to the introductory nature of the course, we will restrict our consideration to problems where $T(x, t)$.

1.2 Lumped system analysis

Sometimes it is possible to greatly simplify a transient heat transfer process by considering the system to be comprised of ‘lumps’. So-called ***Lumped System Analysis*** can be applied in many practical situations where we are dealing for example with the heating or cooling of simple geometrical objects. We have to make a number of simplifying assumptions when setting up our problem. The single most important assumption is that the temperature of the body we are studying is spatially-uniform. This means that the

temperature of the body at any spatial coordinate can be expressed as a function of time only, that is to say $T(t)$. This is demonstrated schematically in Figure 1.

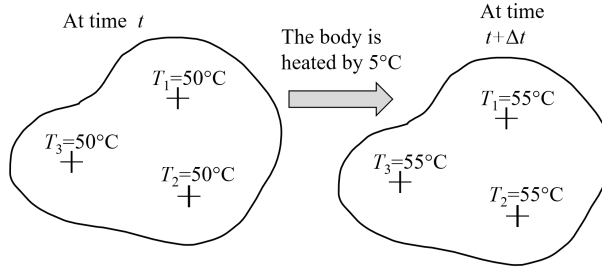


Figure 1: Example of a body with a spatially-uniform temperature distribution at time t (left) and some time later at $t + \Delta t$ (right). Temperature changes are seen to happen equally at all points throughout the body

This is the simplest type of unsteady heat transfer problem that we can consider and using this approach we can answer questions such as how long will it take a given body to reach a certain temperature or conversely, what will the temperature of the body be at a given time?

We will use an example of a small steel ball which has just been removed from a furnace to develop our ideas. A schematic of our problem is illustrated in Figure 2. The steel ball, having mass m and surface area A_s , is cooling outside of the furnace. We assume that the ball is homogeneous, with constant heat capacity C_p , constant thermal conductivity k and temperature $T(t)$. It is placed in an environment with a constant temperature T_∞ and constant heat transfer coefficient h . The initial temperature of the ball is T_i and it is the same at all points (spatially-uniform). Similarly, all temperature changes occur uniformly throughout the body.

To determine the transient temperature response (how the temperature of the ball changes with time) we can relate the rate of heat loss at the surface to the rate of change of the internal energy of the ball. In other words,

$$-hA_s(T - T_\infty)dt = mC_pdT \quad (1)$$

Noting that $m = \rho V$ and $dT = d(T - T_\infty)$ since T_∞ is a constant, we can rearrange equation (1) to get,

$$-\frac{hA_s}{\rho V C_p}dt = \frac{d(T - T_\infty)}{T - T_\infty} \quad (2)$$

Next, we want to integrate from $t = 0$, when $T = T_i$, to any time t at which $T = T(t)$, to get,

$$-\frac{hA_s}{\rho V C_p}t = \ln \left[\frac{(T(t) - T_\infty)}{T_i - T_\infty} \right] \quad (3)$$

Taking the exponential of both sides of equation (3) we are left with our final expression

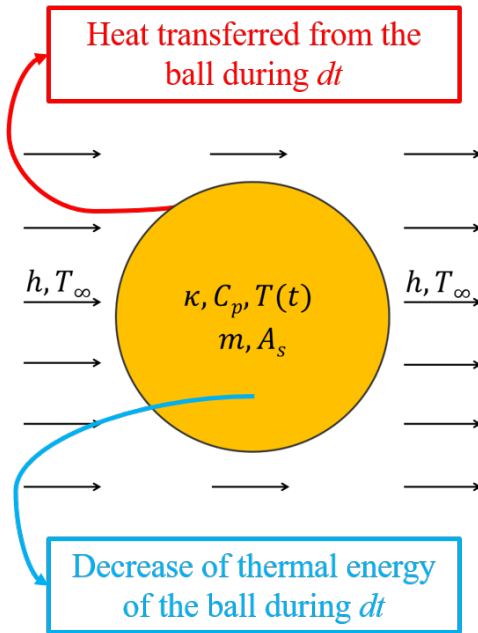


Figure 2: Schematic of a steel sphere cooling outside of a furnace in an environment with constant temperature T_∞ and heat transfer coefficient h

describing temperature change with time,

$$\frac{(T(t) - T_\infty)}{T_i - T_\infty} = e^{-bt} \quad (4)$$

where b is known as the time constant, having units of s^{-1} , and can be further defined as,

$$b = \frac{hA_s}{\rho V C_p} \quad (5)$$

Equation (4) is the governing equation for determining temperature change in lumped system analysis and it also provides a number of further useful insights. First, we see that it allows us to calculate either the temperature $T(t)$ of a body at a given time t or conversely, the time t required for that body to reach a temperature $T(t)$. Second, we see that the temperature $T(t)$ approaches the surrounding temperature T_∞ exponentially, in agreement with Newton's law of heating and cooling. With respect to the time constant b , we see that a large value of b indicates a higher rate of temperature decay. Further, since b is proportional to A_s and inversely proportional to m and C_p of the body, this means that it takes longer to heat or to cool a larger mass, in particular if it also has a large heat capacity. The behaviour of equation (4) is illustrated in Figure 3, using our example of the steel ball cooling outside of the furnace, for different values of the time constant.

In order to determine if it is appropriate to approximate our problem as a lumped system

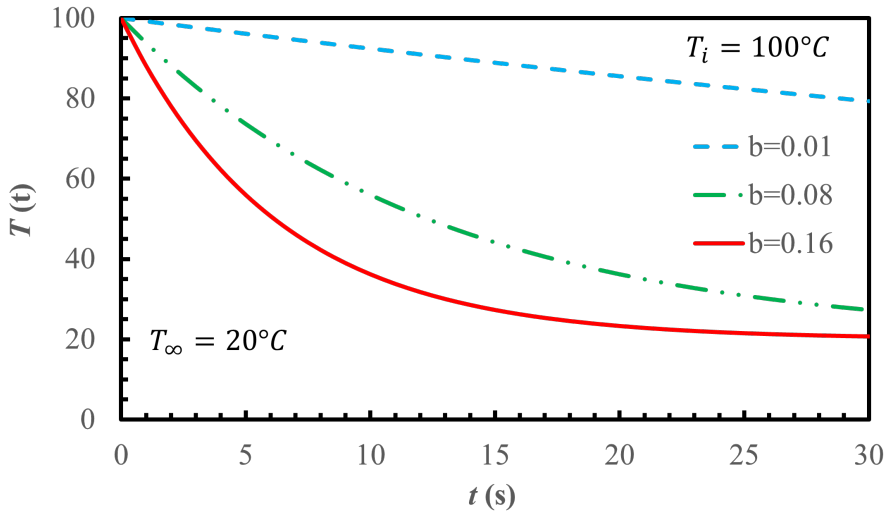


Figure 3: Example of the effect of the time constant b on the cooling rate of an object in a ‘lumped system’. Larger values of b are seen to result in faster rates of cooling between the initial temperature T_i and the final temperature T_∞ . The values chosen in the example are for illustrative purposes only

then we use the dimensionless Biot Number, Bi , which is defined in equation (6) as,

$$Bi = \frac{\text{Conduction resistance within the body}}{\text{Convection resistance at the surface}} = \frac{\left(\frac{L_c}{k}\right)}{\left(\frac{1}{h}\right)} = \frac{hL_c}{k} \quad (6)$$

where L_c is a characteristic length, V is the volume of the body, A_s is the surface area of the body, k is the thermal conductivity of the body and h is the heat transfer coefficient of the external medium.

We see from equation (6) that the Biot number compares the conductive resistance of the body being investigated to the convective resistance of the external medium which surrounds that body. If we want our assumption of a uniform distribution of temperature within the body to hold then we can imagine that the thermal conductivity of the body needs to be high. In other words, the resistance to heat flow within the body should be extremely low. In this way, any changes of temperature experienced at the surface of the body will be communicated throughout the body almost instantaneously. The idea of uniform temperature distribution within the body also becomes less plausible the larger the body is. Therefore, we should expect L_c to have a relatively small value. Taken in combination, a large value of k and a small value for L_c , the Biot number itself should be small and in fact, it is generally accepted that lumped system analysis can only be reliably applied when

$$Bi \leq 0.1 \quad (7)$$

Beyond this limit, the error in the calculations will become unacceptability high. The starting point of any transient heat transfer problem should therefore be the calculation

of the Biot number to determine if we can use the simple lumped system approach.

1.3 Analytical methods

1.3.1 Introduction

As it turns out, in most transient heat transfer problems, the dimensionless Biot number is larger than 0.1 and the lumped system method from section 1.2 cannot be used. In such cases, it is necessary to calculate the temperature distribution across spatial and time domains, i.e. $T(x, y, z, t)$. We start with consideration of the simplest such case where we can assume that the temperature varies with time and one spatial dimension, i.e. $T(x, t)$. There are three commonly encountered geometries where we can make this simplification: (i) the plane wall; (ii) the long cylinder and; (iii) the sphere, as shown in Figure 4.

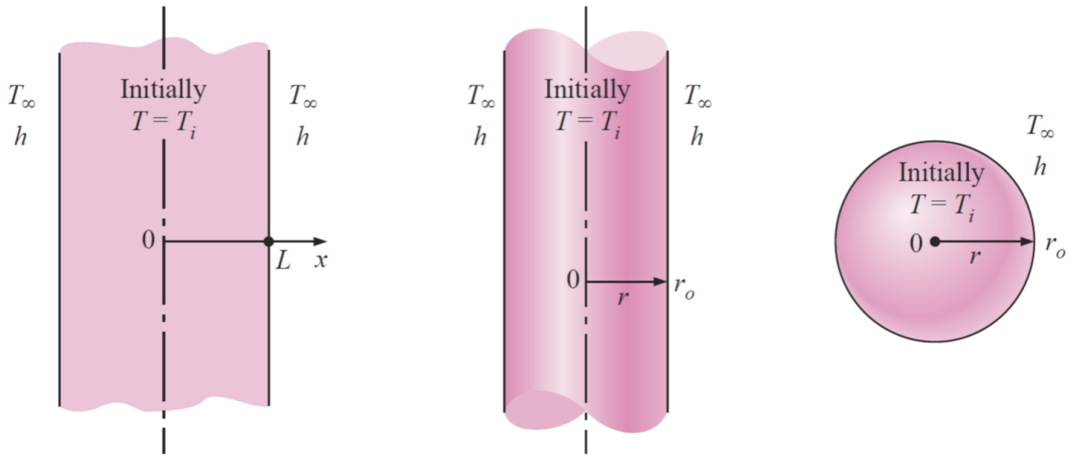


Figure 4: a) Plane wall, b) long cylinder and c) spherical geometries where heat transfer can be considered as one-dimensional (taken from Çengel, 2002, p217)

1.3.2 The plane wall example

Here we will use the example of the plane wall to develop our understanding. Let us assume the plane wall (Figure 4a) has thickness $2L$ with initial uniform temperature distribution $T(x, t = 0) = T_i$. The wall is surrounded by a fluid with constant temperature T_∞ imposing an average convective heat transfer coefficient h . Also, let us assume that the wall height and width are infinite such that the problem can be considered as one-dimensional. Finally, all thermo-physical properties are considered constant, and there is no heat generation. Note, since the geometry is uniform, we can assume an axis of symmetry at $x = 0$ and thus we have a problem of one-dimensional transient heat conduction between $x = 0$ and

$x = L$. To solve it we have to refer back to the heat equation, which for this case we can write as,

$$\frac{\partial^2 T}{\partial x^2} = \frac{1}{\alpha} \frac{\partial T}{\partial t} \quad (8)$$

where $\alpha = k(\rho C_p)^{-1}$ is the heat diffusivity of the material. We also have to define the associated boundary conditions for the problem. First, at $x = 0$, we have a symmetry condition at the centreline of the wall where the temperature gradient must be zero, or in other words,

$$\frac{\partial}{\partial x} T(x = 0, t) = 0 \quad (9)$$

Similarly, for the boundary condition at $x = L$, there has to be a balance between the heat conducted through the material and the heat convected at the surface, which can be described mathematically as,

$$-k \frac{\partial}{\partial x} T(x = L, t) = h(T(x = L, t) - T_\infty) \quad (10)$$

Lastly, we need to define the initial conditions,

$$T(x, t = 0) = T_i \quad (11)$$

In order to solve our heat equation with the associated boundary and initial conditions, it is beneficial for us to first non-dimensionalise the variables. Starting with the temperature

$$\theta = \frac{T - T_\infty}{T_i - T_\infty} \quad (12)$$

which, when substituted back into equation 8, yields,

$$\frac{\partial^2 \theta}{\partial X^2} = \frac{\partial \theta}{\partial \tau} \quad (13)$$

where $X = x/L$ and $\tau = \alpha t / L^2$ are non-dimensional length and time scales, respectively. It is worthwhile noting here that τ is also known as the Fourier number, Fo . As an aside, the dimensionless parameter Fo can be physically interpreted as a measure of the heat conducted through a body relative to the heat stored, such that a larger value of Fo indicates a faster propagation of heat through a body.

The non-dimensional initial conditions are defined as,

$$\theta(X, \tau = 0) = 1 \quad (14)$$

while the non-dimensionalised boundary conditions become,

$$\frac{\partial \theta}{\partial X} = 0 \text{ at } X = 0 \text{ and } \tau > 0 \quad (15)$$

and

$$\frac{\partial \theta}{\partial X} = -Bi \cdot \theta \text{ at } X = 1 \text{ and } \tau > 0 \quad (16)$$

where $Bi = hL/k$ is the non-dimensional Biot number. It is important to be aware that this Biot number is different from the Biot number that we defined previously in section 1.2 on lumped system analysis because here we are using the wall half-thickness L as our characteristic length rather than the V/A_s ratio from before.

By non-dimensionalising, we have reduced our problem from one where the temperature is a function of eight variables i.e. $T = f(x, L, t, k, \alpha, h, T_i, T_\infty)$ to one with $\theta = f(X, Bi, Fo)$, so in general our transient temperature distribution depends only on Bi , Fo and X . An exact analytical solution to this non-dimensionalised heat equation is obtained from the infinite Fourier series expansion,

$$\theta = \sum_{n=1}^{\infty} A_n e^{-\lambda_n^2 \tau} \cos(\lambda_n X) \quad (17)$$

where

$$A_n = \frac{4 \sin \lambda_n}{2\lambda_n + \sin 2\lambda_n}$$

and

$$\lambda_n \tan \lambda_n = Bi$$

So we see that these λ and A coefficients are a function of the Biot number only.

Thankfully, it turns out that for $\tau > 0.2$ the exact solution described by equation (17) can be closely approximated by truncating the infinite series and considering the first term only, which we can write as,

$$\theta = A_1 e^{-\lambda_1^2 \tau} \cos(\lambda_1 X) \quad (18)$$

This is the governing equation that lets us determine the temperature at any spatial location X in our medium at a given time t (for $\tau > 0.2$) and we can obtain our desired solution by either:

1. directly solving equation (18) or,
2. using the transient temperature charts of Heisler.

1.3.3 Analytical method 1 - direct solution of the heat equation

Starting firstly with method 1, this approach involves using look-up tables where the coefficients λ_1 and A_1 from equation (18) have already been determined for a wide range of values of Bi . An extract of the look-up table for a plane wall is shown in Table 1 while the full tables are also available in Appendix A.

Table 1: Coefficients used in the one-term approximate solution of transient 1-D heat conduction for a plane wall of thickness $2L$ (with $Bi = hL/k$)

Bi	λ_1	A_1
0.01	0.0998	1.0017
0.02	0.1410	1.0033
0.04	0.1987	1.0066
0.06	0.2425	1.0098
0.20	0.4328	1.0311
...
∞	1.5708	1.2732

As an example, say we estimate our $Bi = 0.2$ then we can read off Table 1 to get $\lambda_1 = 0.4328$ and $A_1 = 1.0311$. Plugging these values back into equation (18), gives,

$$\theta(X, \tau) = 1.0311e^{-0.4328^2\tau} \cos(0.4328X)$$

which is our desired result because now we have an expression that lets us calculate the temperature at any given location X and time τ and therefore, a solution to our one-dimensional transient heat conduction problem.

As an aside, in this short example directly above we were kind to ourselves and we picked a value of Bi that appeared exactly in the table. That might only happen on rare occasions in practice but not to worry, it is a simple matter of using linear interpolation to find values for A_1 and λ_1 which do not appear in the table.

1.3.4 Analytical method 2 - transient temperature charts of Heisler

An alternative approach is to use transient temperature charts developed by M.P. Heisler in the late 1940's. For the prescribed plane wall geometry that we have been considering, there are two charts that we need to use to determine the temperature at a given time and

spatial location. The first chart determines the temperature T_0 at the centreline of our plane wall, at a given time t . The second chart is then used to determine the temperature at other locations at that same time t for our given T_0 . Similar to method 1, we first need to know Bi for our particular problem. The Heisler charts for our plane wall geometry are shown in Figure 5.

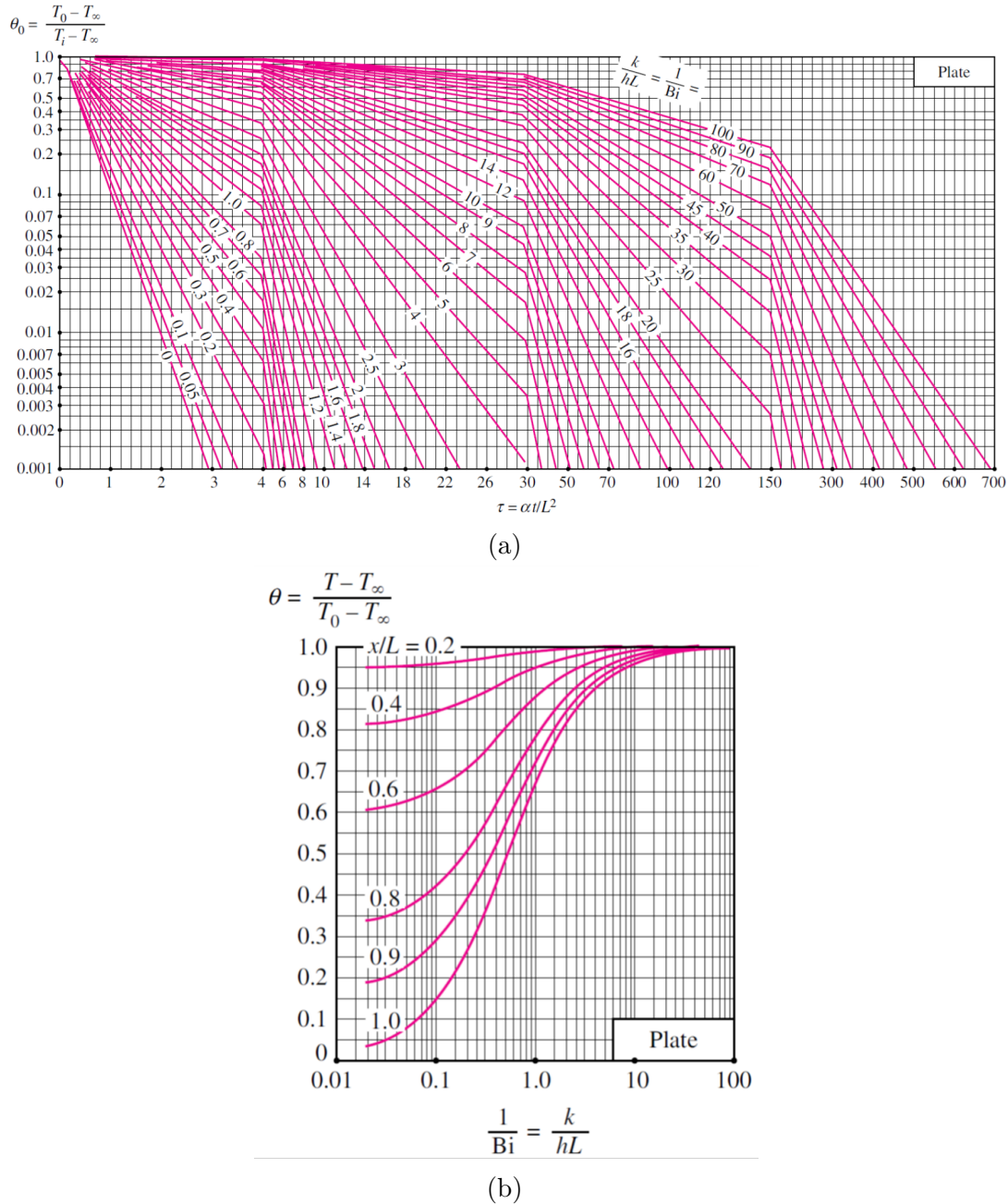


Figure 5: a) Midplane temperature chart and b) temperature distribution chart for a plane wall geometry after Heisler, 1947 (taken from Çengel, 2002, p220)

As an example of how to use these charts, let us start by saying that we have a Biot number of $Bi=0.25$ and we want to know T_0 at say $\tau=22$. Then we can read from the

chart in Figure 5a that $\theta = 0.065$. We can then find T_0 from the relation on the chart,

$$\theta_0 = \frac{T_0 - T_\infty}{T_i - T_\infty}$$

for any given initial temperature T_i and constant external temperature, T_∞ . Next, say we want to know the temperature at the edge of the plate i.e. $x/L=0$, then we can use the chart in Figure 5b to find θ (for our given $Bi=0.25$ and the T_0 that we determined from chart 1) from which we can then find T by rearranging the expression,

$$\theta = \frac{T - T_\infty}{T_0 - T_\infty}$$

1.3.5 Calculating heat transfer

In addition to $T(x, t)$, we can also make some estimations of the heat transfer Q . Starting with the maximum amount of heat that can be transferred to/from our plane wall we see that it is constrained primarily by the difference between the initial temperature T_i and the external temperature T_∞ ,

$$Q_{\max} = mC_p(T_\infty - T_i) = \rho V C_p(T_\infty - T_i) \quad (19)$$

On the other hand, the amount of heat Q (per unit volume) transferred at a time t is,

$$Q = \int_V \rho C_p [T(x, t) - T_i] dV \quad (20)$$

Assuming ρC_p remains constant, we can form the dimensionless ratio,

$$\frac{Q}{Q_{\max}} = \frac{\int_V \rho C_p [T(x, t) - T_i] dV}{\rho V C_p (T_\infty - T_i)} = \frac{1}{V} \int_V (1 - \theta) dV \quad (21)$$

which, when integrated, yields our desired expression,

$$\frac{Q}{Q_{\max}} = 1 - \theta_0 \frac{\sin \lambda_1}{\lambda_1} \quad (22)$$

where $\theta_0 = A_1 e^{-\lambda_1^2 \tau}$. Again, we can choose from one of two ways to solve equation (22), either directly, using the look-up tables for the coefficients A_1 and λ_1 or graphically, using the charts developed by Gröber.

The solution strategy using the look-up tables is broadly similar to what was done for solving equation (18) in section 1.3.3. Once Bi is known for our problem we can obtain

our values of A_1 and λ_1 and subsequently, θ_0 , before plugging these back into equation (22) to get our desired heat transfer rate.

The graphical approach is also very similar to what was described previously in section 1.3.4 only now instead of using the Heisler charts, which deal with temperatures, we are going to use a so-called Gröber chart, which relates to heat transfer rates. An example of a Gröber chart for our plane-wall is given in Figure 6. To use the chart we simply need to calculate our value for Bi and τ (or Fo) and read off the corresponding value for Q/Q_{\max} .

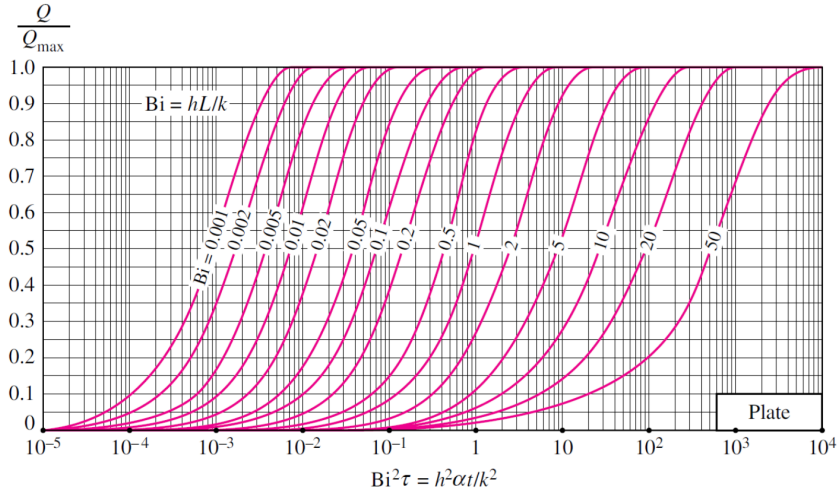


Figure 6: Gröber's heat transfer chart for a plane wall geometry (taken from Cengel, 2002, p220)

1.3.6 Different geometries

Up to now our focus has been solely on the plane wall example. However, it was alluded to in section 1.3.1 that analytical solutions could be obtained for two other simple geometrical arrangements, namely the long cylinder and the sphere (see Figure from 1.3.1). Here we will compare the equivalent governing equations for the plane-wall, cylinder and sphere cases. Starting with the governing equation for determining temperature, we have

$$\theta_{wall} = A_1 e^{-\lambda_1^2 \tau} \cos(\lambda_1 X) \quad (23)$$

$$\theta_{cyl} = A_1 e^{-\lambda_1^2 \tau} J_0(\lambda_1 R) \quad (24)$$

$$\theta_{sph} = A_1 e^{-\lambda_1^2 \tau} \frac{\sin(\lambda_1 R)}{\lambda_1 R} \quad (25)$$

where J_0 is zeroth-order Bessel function of the first kind and $R = r/r_0$ is the non-dimensional radial coordinate. While for determining heat transfer we have,

$$\left(\frac{Q}{Q_{\max}} \right)_{wall} = 1 - \theta_0 \frac{\sin \lambda_1}{\lambda_1} \quad (26)$$

$$\left(\frac{Q}{Q_{\max}}\right)_{cyl} = 1 - 2\theta_0 \frac{J_1(\lambda_1)}{\lambda_1} \quad (27)$$

$$\left(\frac{Q}{Q_{\max}}\right)_{sph} = 1 - 3\theta_0 \frac{\sin \lambda_1 - \lambda_1 \cos \lambda_1}{\lambda_1^3} \quad (28)$$

where J_1 is first-order Bessel function of the first kind and $\theta_0 = A_1 e^{-\lambda^2 \tau}$ as defined previously.

Now just by a quick visual comparison of the equations we can see that temperature and heat transfer problems for spheres can be solved in an identical manner to that of the plane-wall. Namely, once we determine the Biot number for our problem then it is simply a matter of then reading off our values of A_1 and λ_1 from the look-up tables or using the corresponding Heisler charts.

The same is true for the case of the cylinder however with one simple additional step. We see that there are two new terms J_0 and J_1 . Look-up tables have also been developed for J_0 and J_1 so it is a simple matter to read off the required values. It is important to note that J_0 and J_1 are functions and in order to get their values from the tables we first have to calculate the argument of those functions. By inspection of equations (24) and (27) we see that the argument of J_0 is $\lambda_1 R$ while for J_1 it is just λ_1 . The look-up tables for J_0 and J_1 are shown in Appendix A.

1.3.7 Some further comments

Full Heisler and Gröber charts (and all other look-up tables) for spherical, cylindrical and plane-wall geometries are available online and from most heat transfer textbooks. As noted, they are also listed in Appendices A and B at the end of these notes. The following are some conditions for using the Heisler and Gröber charts that you should be aware of:

1. the body is initially at a uniform temperature;
2. the temperature of the surroundings is constant and uniform;
3. the convective heat transfer coefficient is constant and uniform and;
4. there is no heat generation in the body.

1.4 Numerical methods

1.4.1 Introduction

The analytical methods introduced in the previous section are easy to apply through either direct solution of the heat equation or the Heisler and Gröber charts. These methods are however mostly constrained to one-dimensional and simple geometries. Numerical methods offer a great alternative to solve partial differential equations (PDEs) by replacing differential equations with algebraic equations. Many different numerical techniques are available but among the most common in practice are so-called Finite Difference Methods (FDM) and this is where we will focus our attention. Furthermore, while numerical methods can be applied to solve fully three-dimensional heat transfer problems i.e. $T(x, y, z, t)$, due to the introductory nature of the course we will confine ourselves to one-dimensional problems of type $T(x, t)$.

1.4.2 Discretising the domain

One of the most important steps in the successful implementation of FDM is the correct discretisation of our domain where we want to compute our temperature distribution. Keeping things simple, let us consider our plane-wall example from section 1.3. As shown in Figure 7, we split the domain into n grid points. These are equally spaced in increments of Δx (grid step). The grid points at $i = 1$ and $i = n$ are known as the boundary nodes, while all others are interior nodes. Our goal is to solve the heat equation at each of the grid points in order to obtain the temperature distribution between $x = 0$ and $x = L$.

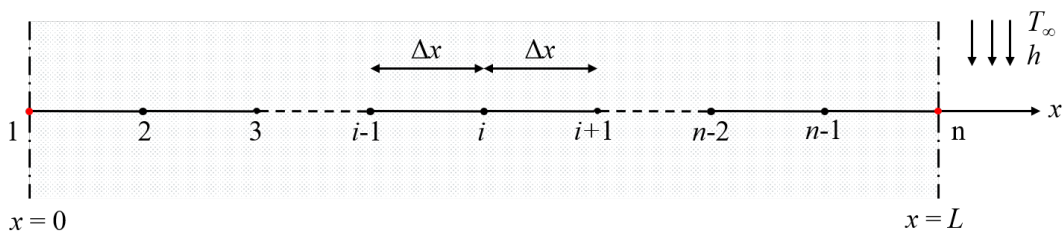


Figure 7: A discrete set of grid points, equally spaced in increments of Δx across a plane wall. In this example, grid points $i = 1$ and $i = n$ are the boundary nodes while all other nodes are interior nodes

1.4.3 Discretising the heat equation

Now that we have established a suitable domain, we need to establish an appropriate discrete version of the heat equation which we can then solve at each of the grid points in

our domain. Recall the one-dimensional transient heat equation,

$$\frac{\partial^2 T}{\partial x^2} = \frac{1}{\alpha} \frac{\partial T}{\partial t} \quad (29)$$

The first step in applying FDM is to replace the derivatives in equation (29) with differences. So starting with the time term we get,

$$\frac{\partial T_i}{\partial t} = \frac{T_i^{j+1} - T_i^j}{\Delta t} \quad (30)$$

where $\Delta t = t^{j+1} - t^j$ is the time-step size. Similarly, the diffusion term can be discretised in space as follows,

$$\alpha \frac{\partial^2 T}{\partial x^2} = \alpha \frac{T_{i+1} - 2T_i + T_{i-1}}{\Delta x^2} \quad (31)$$

where $\Delta x = x_{i+1} - x_i$ is the grid-step size. Recombining and rearranging equations (30) and (31) yields the full discretised version of our one-dimensional heat equation as,

$$T_i^{j+1} = T_i^j + \frac{\alpha \Delta t}{\Delta x^2} (T_{i+1}^j - 2T_i^j + T_{i-1}^j) \quad (32)$$

Note, in equation (32) we have used subscript indices i to represent increments in the spatial domain and superscript indices j to represent increments in the time domain and this is also demonstrated graphically in Figure 8. We can use this expression to calculate the temperature **at any interior node** along our domain (e.g. $i = 2, \dots, n - 1$) and at any particular time step ($j = 1, \dots, m$). Note that the time step at $j = 1$ corresponds to our initial condition ($t = 0$) while the boundary nodes at $i = 1$ ($x = 0$) and $i = n$ ($x = L$) are treated separately, as discussed next.

1.4.4 Discretised boundary conditions

The transient problem may be subject to two different types of boundary conditions, Dirichlet or Neumann. When Dirichlet boundary conditions are imposed we are specifying a fixed value (or function) at the boundary node(s), or in other words

$$T_1^{j+1} = T_1^j = \Psi_1 \quad (33)$$

and/or

$$T_n^{j+1} = T_n^j = \Psi_2 \quad (34)$$

where Ψ_1 and Ψ_2 is either a fixed constant or function. Whereas, when Neumann boundary conditions are imposed then we are specifying a prescribed flux at the boundary. So for example, with the plane-wall problem that we have been working through so far, we have

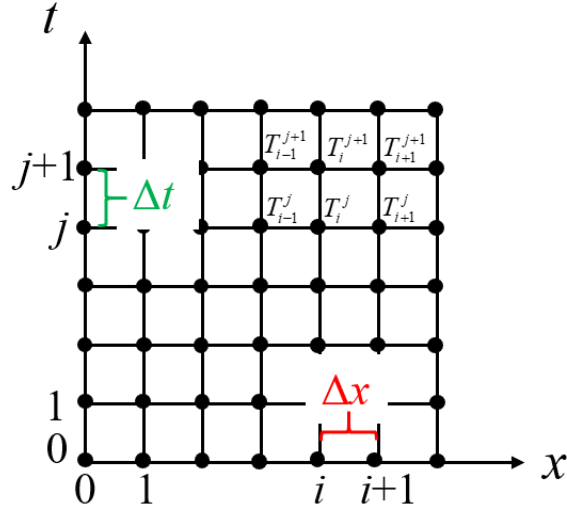


Figure 8: Example of the ‘2D’ grid set up for solving the one-dimensional transient heat equation. The horizontal axis is used to represent changes in space (subscript i , increments of Δx) while the vertical axis shows changes in time (subscript j , increments of Δt)

the following boundary condition that

$$-k \frac{\partial}{\partial x} T(x_n, t_j) = h [T(x_n, t_j) - T_\infty] \quad (35)$$

When translated to our required discretised form in the heat equation reads as,

$$T_n^{j+1} = T_n^j + \frac{h\Delta t}{\rho C_p} (T_n^j - T_\infty) + \frac{k\Delta t}{\rho C_p \Delta x} (T_n^j - T_{n-1}^j) \quad (36)$$

These different boundary conditions are also shown in Figure 9.

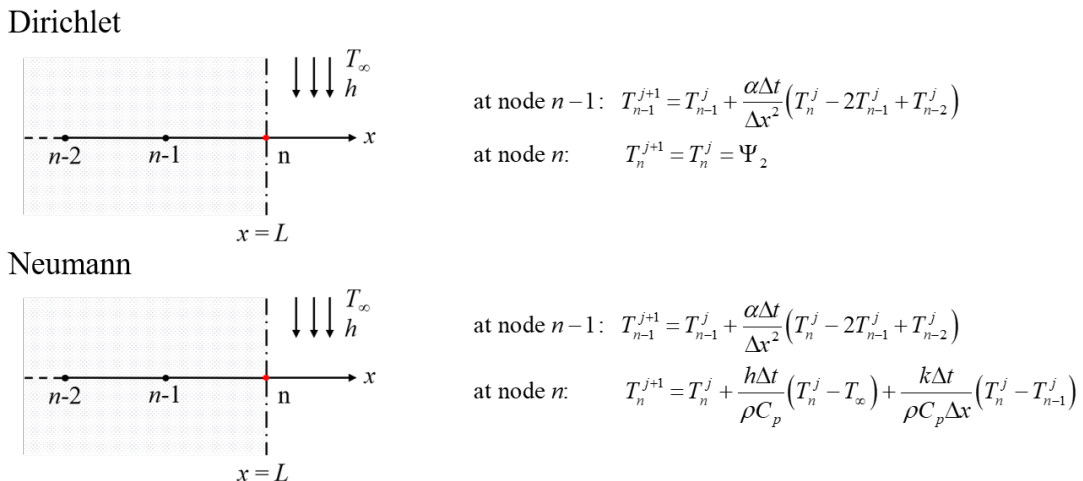


Figure 9: Example of how Dirichlet and Neumann boundary conditions are applied in a one-dimensional problem with convective heat transfer at the boundary

1.4.5 Stability criteria

In our application of FDM e.g. equation (32), the new temperature, at time-step t_{j+1} , is obtained from the previous known temperature at time-step t_j . This is therefore considered to be a *forward-difference* approximation to the derivatives and this method is most commonly referred to as the *explicit* method. The explicit method is straightforward to use, however it is not unconditionally stable and its validity is dictated by the time-step size, Δt . If the time-step is not sufficiently small, the solutions obtained by the explicit method may oscillate and diverge from the actual solution. In order to avoid these numerical oscillations t must be kept below a certain upper limit established by the **stability criterion**, based on the Fourier number, which for one-dimensional problems is

$$Fo = \frac{\alpha \Delta t}{\Delta x^2} \leq \frac{1}{2} \quad (37)$$

Further reading

- Çengel, Y.A. (2002). *Heat Transfer: A Practical Approach*, 2nd Edition, McGraw-Hill: Chapters 4-5
- Holman, J.P. (2010). *Heat Transfer*, 10th Edition, McGraw-Hill: Chapter 4
- Incropera, F.P., DeWitt, D.P., Bergman, T.L., Lavine, A.S. (2006). *Introduction to Heat Transfer*, 6th Edition, John Wiley & Sons: Chapter 5
- Karwa, R. (2020). *Heat and Mass Transfer*, 2nd Edition, Springer: Chapter 6
- Theodore, L. (2011). *Essential Engineering Calculations Series: Heat Transfer Applications for the Practicing Engineer*, John Wiley & Sons: Chapter 8

A Look-up tables

TABLE 4-1

Coefficients used in the one-term approximate solution of transient one-dimensional heat conduction in plane walls, cylinders, and spheres ($\text{Bi} = hL/k$ for a plane wall of thickness $2L$, and $\text{Bi} = hr_o/k$ for a cylinder or sphere of radius r_o)

Bi	<i>Plane Wall</i>		<i>Cylinder</i>		<i>Sphere</i>	
	λ_1	A_1	λ_1	A_1	λ_1	A_1
0.01	0.0998	1.0017	0.1412	1.0025	0.1730	1.0030
0.02	0.1410	1.0033	0.1995	1.0050	0.2445	1.0060
0.04	0.1987	1.0066	0.2814	1.0099	0.3450	1.0120
0.06	0.2425	1.0098	0.3438	1.0148	0.4217	1.0179
0.08	0.2791	1.0130	0.3960	1.0197	0.4860	1.0239
0.1	0.3111	1.0161	0.4417	1.0246	0.5423	1.0298
0.2	0.4328	1.0311	0.6170	1.0483	0.7593	1.0592
0.3	0.5218	1.0450	0.7465	1.0712	0.9208	1.0880
0.4	0.5932	1.0580	0.8516	1.0931	1.0528	1.1164
0.5	0.6533	1.0701	0.9408	1.1143	1.1656	1.1441
0.6	0.7051	1.0814	1.0184	1.1345	1.2644	1.1713
0.7	0.7506	1.0918	1.0873	1.1539	1.3525	1.1978
0.8	0.7910	1.1016	1.1490	1.1724	1.4320	1.2236
0.9	0.8274	1.1107	1.2048	1.1902	1.5044	1.2488
1.0	0.8603	1.1191	1.2558	1.2071	1.5708	1.2732
2.0	1.0769	1.1785	1.5995	1.3384	2.0288	1.4793
3.0	1.1925	1.2102	1.7887	1.4191	2.2889	1.6227
4.0	1.2646	1.2287	1.9081	1.4698	2.4556	1.7202
5.0	1.3138	1.2403	1.9898	1.5029	2.5704	1.7870
6.0	1.3496	1.2479	2.0490	1.5253	2.6537	1.8338
7.0	1.3766	1.2532	2.0937	1.5411	2.7165	1.8673
8.0	1.3978	1.2570	2.1286	1.5526	2.7654	1.8920
9.0	1.4149	1.2598	2.1566	1.5611	2.8044	1.9106
10.0	1.4289	1.2620	2.1795	1.5677	2.8363	1.9249
20.0	1.4961	1.2699	2.2880	1.5919	2.9857	1.9781
30.0	1.5202	1.2717	2.3261	1.5973	3.0372	1.9898
40.0	1.5325	1.2723	2.3455	1.5993	3.0632	1.9942
50.0	1.5400	1.2727	2.3572	1.6002	3.0788	1.9962
100.0	1.5552	1.2731	2.3809	1.6015	3.1102	1.9990
∞	1.5708	1.2732	2.4048	1.6021	3.1416	2.0000

TABLE 4-2

The zeroth- and first-order Bessel functions of the first kind

ξ	$J_0(\xi)$	$J_1(\xi)$
0.0	1.0000	0.0000
0.1	0.9975	0.0499
0.2	0.9900	0.0995
0.3	0.9776	0.1483
0.4	0.9604	0.1960
0.5	0.9385	0.2423
0.6	0.9120	0.2867
0.7	0.8812	0.3290
0.8	0.8463	0.3688
0.9	0.8075	0.4059
1.0	0.7652	0.4400
1.1	0.7196	0.4709
1.2	0.6711	0.4983
1.3	0.6201	0.5220
1.4	0.5669	0.5419
1.5	0.5118	0.5579
1.6	0.4554	0.5699
1.7	0.3980	0.5778
1.8	0.3400	0.5815
1.9	0.2818	0.5812
2.0	0.2239	0.5767
2.1	0.1666	0.5683
2.2	0.1104	0.5560
2.3	0.0555	0.5399
2.4	0.0025	0.5202
2.6	-0.0968	-0.4708
2.8	-0.1850	-0.4097
3.0	-0.2601	-0.3391
3.2	-0.3202	-0.2613

(from Çengel, 2002, p219)

B Heisler and Gröber charts

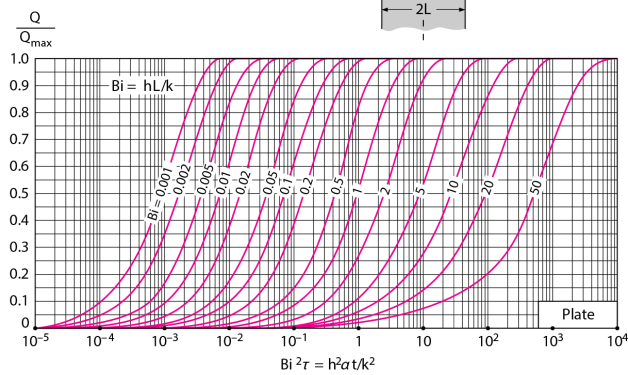
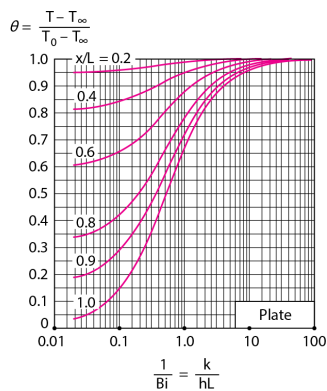
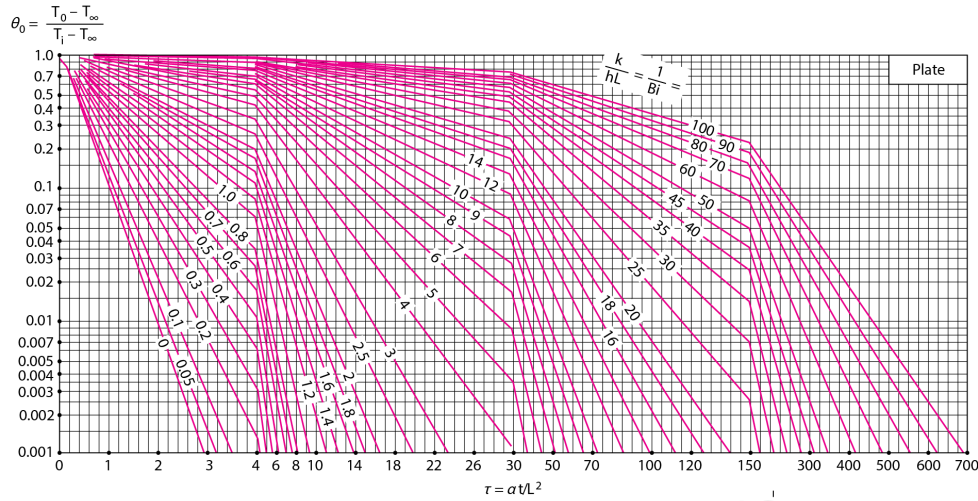
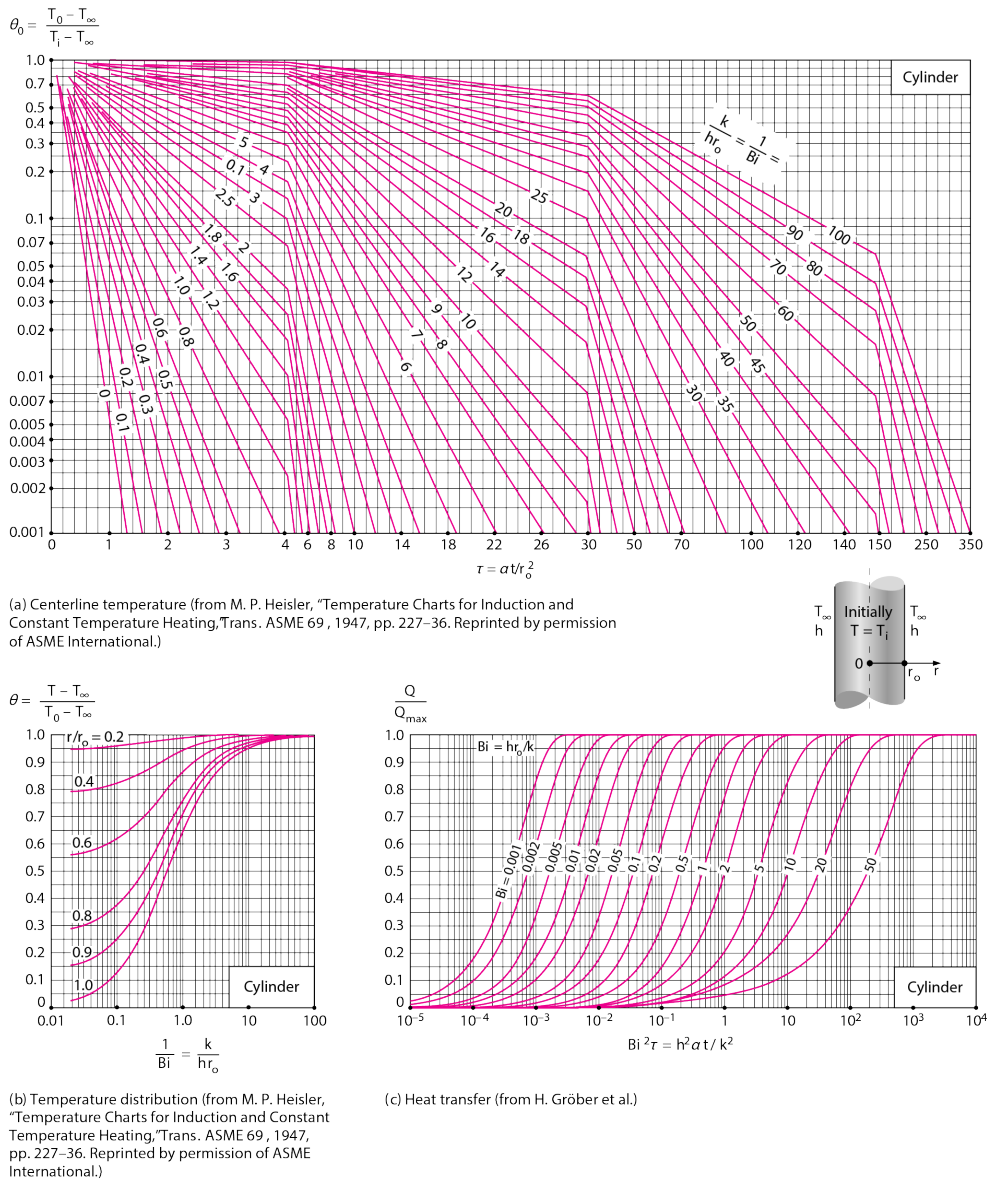


FIGURE 4-15
Transient temperature and heat transfer charts for a plane wall of thickness $2L$ initially at a uniform temperature T_i subjected to convection from both sides to an environment at temperature T_∞ with a convection coefficient h .

(from Çengel, 2002, p220)



(from Çengel, 2002, p221)

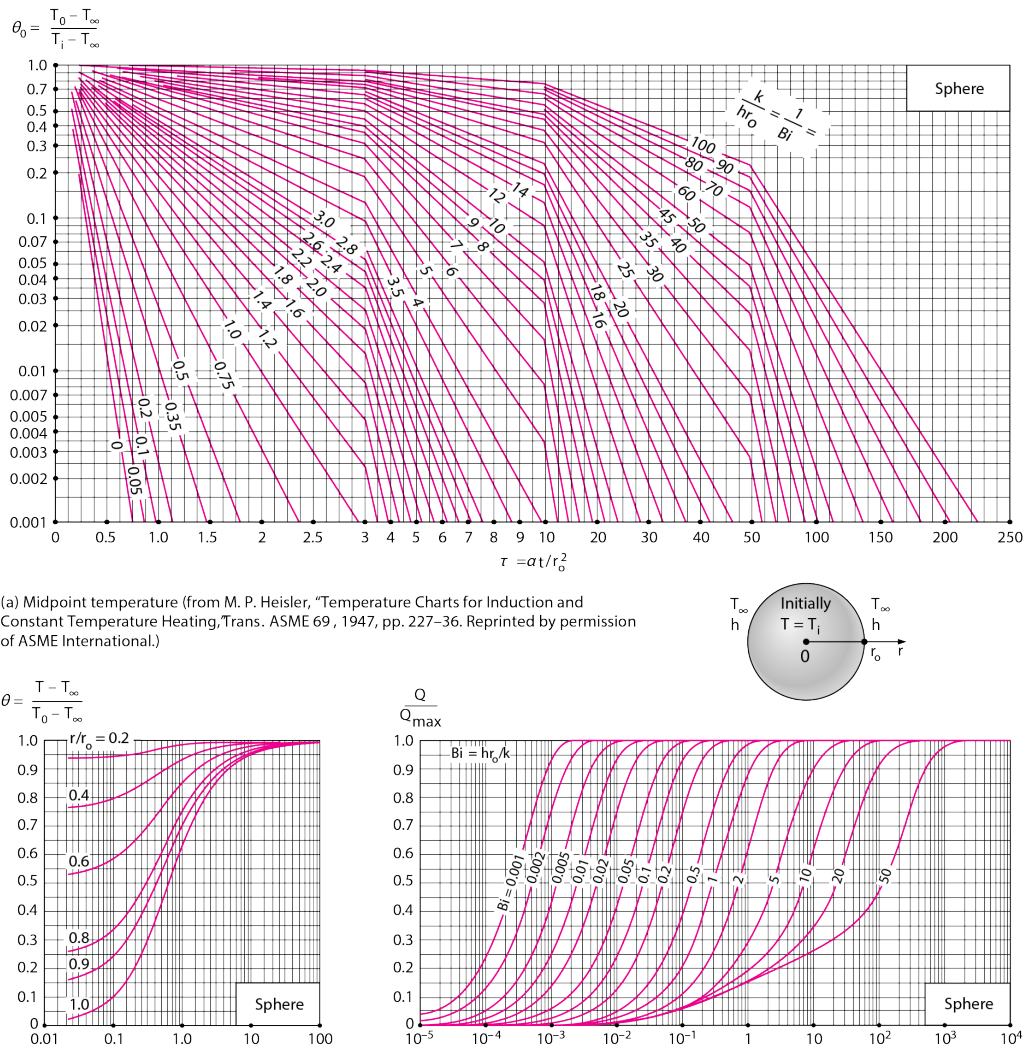


FIGURE 4-17

Transient temperature and heat transfer charts for a sphere of radius r , initially at a uniform temperature T_i subjected to convection from all sides to an environment at temperature T_∞ with a convection coefficient of h .

(from Çengel, 2002, p222)